18th International Conference on Protection & Automation in Power System
Shahrood University of Technology
January 9, 2024 - January 10, 2024

Fault Detection, Classification, and Location in VSC-HVDC Systems Using Metaheuristic Optimized ANFIS and Hilbert Huang Transform Method

Ehsan Akbari
Dep. of Electrical Engineering,
Mazandaran University of Science and Technology,
Babol, Iran
e.akbari@ustmb.ac.ir

Milad Samady Shadlu
Dep. of Electrical Engineering,
Young Researchers and Elite Club, Bojnourd Branch, Islamic Azad University,
Bojnourd, Iran
milad.samady@yahoo.com

***Abstract*—Identifying, classifying, and locating various faults in HVDC networks can significantly reduce maintenance costs in these systems. For this reason, intelligent methods for detecting and locating faults with high accuracy and speed have recently been the focus of system planners and operators. This paper proposes an intelligent fault detection, classification, and location framework based on the adaptive neuro-fuzzy inference system (ANFIS), whose training and testing data are generated using the Hilbert-Huang (HH) transform-based feature extraction method. DC link current is measured as a fault signal, and its statistical characteristics are extracted employing HH transform. Furthermore, for training and testing ANFIS, a meta-heuristic algorithm with dynamic search capability and high convergence speed called the Modified Cuckoo Search (MCS) Algorithm is used. In addition, two conventional training methods, i.e., least square estimation (LSE) and gradient descent (GD), are applied to train ANFIS, and its performance is compared with the MCS algorithm. The numerical analysis results validate the accuracy of 97.37% in classification and 98.39% in location using the proposed framework. Additionally, the comparative study confirms a 12.18% reduction in mean squared error (MSE) value compared with the best result obtained in the literature.**

Keywords-Fault detection, classification, and location; VSC-HVDC system; Optimized ANFIS; Modified cuckoo search algorithm; Hilbert-Huang transform.

I. Introduction

VSC-HVDC networks are exposed to various faults due to their long length and high power transmission, which may cause heavy damage to the network if not identified and located accurately [1]. From the point of view of the data acquisition method, fault detection and location strategies used in the HVDC network are divided into three general categories: parameter-based or model-based methods, frequency component-based methods, and knowledge-based methods [2]. Traditional fault detection schemes such as the time-domain impedance-based [3] and the virtual impedance-based methods [4] belong to the parameter-based approaches. These methods suffer from high estimation error and dependency of the estimation accuracy on the network parameters. To cope with these challenges, frequency component-based strategies have been presented, the most common of which is Gap Frequency Spectrum Analysis (GAP) [5] and widely used methods based on traveling waves (TWs) [6]-[10]. On the other hand, the accuracy of the traveling wave methods depends on the installation location of the fault locator and is affected by the front of TWs [11]. In addition, the performance of TW-based methods is weakened by changing the fault resistance and line parameters [12].

In order to address these challenges, knowledge-based intelligent fault detection models have been proposed, the most common of which is the adaptive neuro-fuzzy inference system (ANFIS). Due to the ability of training using the data obtained from the system, ANFIS-based methods are not sensitive to fault parameter changes; hence, they exhibit high accuracy and speed in fault detection and location [13]. In addition, they can perform fault classification accurately due to the ability to train by data obtained from different fault scenarios [14]. However, ANFIS-based estimation methods have two fundamental limitations: first, the ANFIS training strategy significantly affects its estimation accuracy, and second, depending on how much information the training data contains about the fault, the performance of the ANFIS framework is affected [15]. To solve the first problem, heuristic and meta-heuristic algorithms are applied for ANFIS training, which considerably improves its estimation accuracy [16], [17]. In the case of the second problem, feature extraction techniques can be employed to extract useful features from the fault signal [18]. Numerous

feature extraction techniques have been introduced in the literature [19]. Among these, the wavelet transform (WT) has been widely exploited in the literature to extract the features of the fault signal in various applications [20]-[24]. However, the main drawback of this technique is choosing the mother wavelet, which affects the number of resolution levels and the number of sampling features. According to the studies, the Daubechies-family mother wavelets are preferred for fault signals with severe changes [25]. However, these mother wavelets result in high-resolution levels, which causes an exponential increase in the number of samples; hence, it is inevitable to use feature reduction methods such as PCA in a combined form [26]. This will increase the complexity of the fault detection and classification scheme and its execution time.

To cope with these shortages, this paper proposes a fault detection, classification, and location model based on optimized ANFIS and Hilbert-Huang transform-based feature extraction technique. In the HH transform technique, the Fourier spectrum of the real and imaginary components of the Hilbert function of the fault signal is obtained, and the statistical characteristics are calculated according to these spectra. Then, the extracted feature matrix is applied for ANFIS training. Next, the ANFIS-based fault detection, classification, and location model are trained and tested utilizing the features obtained from the HH transform. To determine the optimal design of ANFIS, a modified cuckoo search (MCS) algorithm is used. The advantage of the HH transform-based feature extraction technique is that it is applicable for all fault types, and there is no limitation on the initial parameters selection, unlike the WT-based methods. In addition, because the Hilbert function provides a unique spectrum for each type of fault, a rich set of statistical features can be extracted, which improves the performance of the ANFIS-based classifier. Furthermore, the performance of the MCS optimization algorithm is compared with other conventional ANFIS training methods, i.e., least square estimation (LSE) and gradient descent (GD).

The paper proceeds as follows. Section II describes the proposed fault detection, classification, and location framework. Section II provides the numerical and comparative study results, and Section IV finalizes with the conclusions.

II. The Proposed Fault Detection, Classification, and Location Strategy

The proposed framework is depicted in Fig. 1. In this figure, the first block performs fault detection based on the HH transform feature extraction technique, and the second block performs fault classification and location utilizing the optimal ANFIS. The features extracted from the fault signal include mean value, standard deviation, and norm entropy calculated from the real and imaginary Hilbert spectra. Fig. 2 illustrates the structure of ANFIS with the mentioned three features as inputs. For ANFIS optimization, the optimal values of two parameters, antecedent or premise and conclusion or consequent, are obtained. In this study, a recently introduced meta-heuristic algorithm called the modified cuckoo search (MCS) algorithm is exploited to optimize ANFIS. This algorithm will be explained in the next subsection.

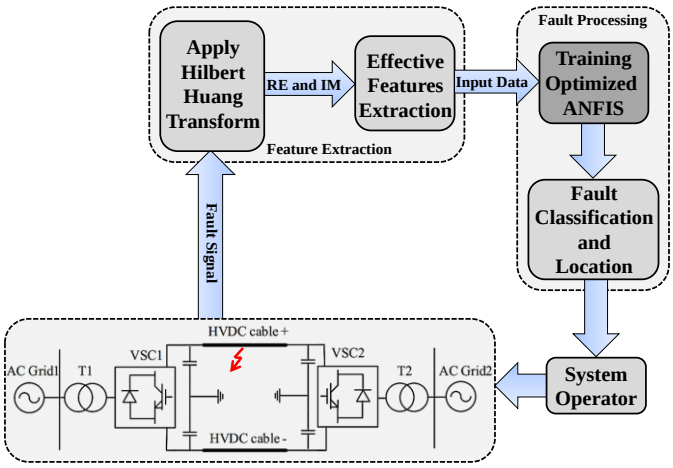

Figure 1. Structure of the proposed model

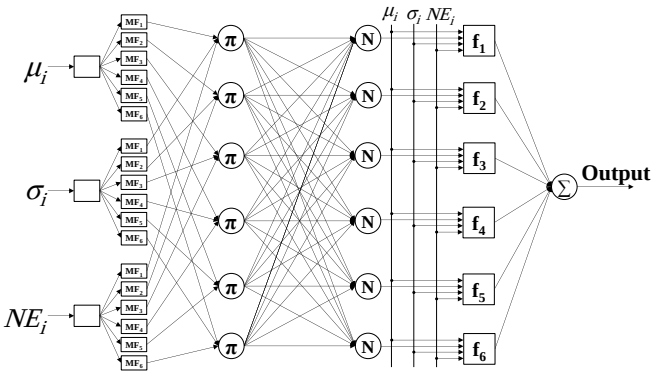

Figure 2. ANFIS structure with three inputs

A. ANFIS Optimization Algorithm

In this paper, the modified cuckoo search (MCS) optimization algorithm is utilized to determine the optimal parameters of ANFIS. The use of the CS algorithm in the field of optimization was proposed by Yang and Deb in 2009 [27]. This algorithm is based on the parasitic behavior of broods, which is observed in some cuckoo species. This type of bird performs a Levy random flight to find the destination nest for laying eggs, which is the exploration stage in the search space. Levy flight is expressed mathematically as follows:

$$Levy\ (\lambda) = t^{-\lambda}, \quad 1 < \lambda \le 3 \tag{1}$$

where λ is the mathematical expectation of nest selection at time step t. The following rules are valid for the CS algorithm:

- Each cuckoo lays one egg at a time and places it in a randomly selected nest.
- The best nest containing the highest quality eggs is selected as the optimal response.
- The number of host nests is fixed. Also, the probability of finding cuckoo eggs by the host bird is represented by $P_\alpha \epsilon (0,1)$.

This algorithm comprises two sets of solutions obtained during two stages: Levy flights and discarding stage [28]. After selecting the proper nest, the promising solution per nest is

chosen according to the conditions expressed in (2). Each nest *s* includes two solutions (eggs), *Xs* and *Ys*, where only one is retained and the other discarded during the discarding stage.

$$Z_s = \begin{cases} Y_s & if\ \ FF(Y_s) > FF(X_x) \\ X_x & otherwise \end{cases} \quad (2)$$

where *FF*(.) indicates the fitness function value corresponding to each solution. To modify the classical CS algorithm, in this step, a three-mode mutation procedure is applied to the selected solution to improve its quality according to the following conditions:

$$U_s = \begin{cases} Z_s + rand\,(Z_{r1} - Z_{r2}),\ if\ \ (\Delta Z_s > \Delta_{mean}) \\ Z_s + rand\,(Z_{r1} - Z_{r2} + Z_{r3} - Z_{r4}),\ if\ \ (\Delta Z_s < \Delta_{mean}\ \&\ rand_{U_s} > 0.5) \\ Z_s + rand\,(Z_{best} - Z_s + Z_{r1} - Z_{r2}),\ if\ \ (\Delta Z_s < \Delta_{mean}\ \&\ rand_{U_s} < 0.5) \end{cases} \quad (3)$$

where Z_{best} indicates the best solution among all solutions associated with all nests, and Z_{ri} (i=1,2,3,4) represents randomly selected solutions. $rand_{Us}$ represents a randomly produced value in the range of (0,1) for solution U_s. These mutation modes exhibit three search strategies, while the condition of employing each strategy is determined by comparing two indices ΔZ_s and Δ_{mean} defined in (4) and (5).

$$\Delta Z_s = \left| \frac{FF(Z_s)}{FF(Z_{best})} - 1 \right| \quad (4)$$

$$\Delta_{mean} = \left| \frac{\sum_{s=1}^{N_{nest}} FF(Z_s)}{N_{nest} \times FF(Z_{best})} - 1 \right| \quad (5)$$

where ΔZ_s and Δ_{mean} denote the individual fitness index and the average fitness index, respectively. The pseudo-code of the MCS algorithm is presented in **"Algorithm 1"**.

Algorithm 1. Pseudo-code of MCS optimization algorithm

1. Determine the objective function $f(X)$, $X=(x_1,\ldots,x_d)^T$
2. Specify the initial population corresponding to n nests, X_i (i=1,...,n)
3. Repeat the following steps until t < Maximum Iteration:
4. Select cuckoo i randomly according to the Levy flight criterion.
5. Calculate the fitness function, FF_i, for the selected cuckoo.
6. Choose nest α among n nests randomly and calculate FF_j for the selected nest.
7. If $FF_i > FF_j$,
8. Replace j with a new solution.
9. Calculate the probability P_α for nest j.
10. Choose the nest with the lowest P_α as the best solution.
11. Execute the discarding phase for the selected nest according to Eq. (2).
12. Apply the three-mode mutation procedure to the selected solution according to Eq. (3).
13. Obtain the global best solution.
14. End

B. Feature Extraction Technique

In this section, the feature extraction technique based on HH transform is explained. This method is implemented by applying the empirical mode decomposition (EMD) [29] on the fault signal so that the intrinsic mode functions (IMFs) are extracted from the original signal. By applying the Hilbert function to each IMF, a pair of real and imaginary components is obtained, and by averaging over all IMFs, signals containing real (RE) and imaginary (IM) samples are acquired. Next, the three statistical indices, i.e., mean value (μ), standard deviation (σ), and norm entropy (*NE*) defined respectively in (6) to (8), are calculated for each pair of signals containing RE and IM samples.

$$\mu_i = \frac{1}{N} \sum_{j=1}^{N} c_{ij} \quad (6)$$

$$\sigma_i = \left(\frac{1}{N} \sum_{j=1}^{N} \left(c_{ij} - \mu_i \right)^2 \right)^{\frac{1}{2}} \quad (7)$$

$$NE_i = \sum_{j=1}^{N} c_{ij}^P \qquad P \geq 1 \quad (8)$$

In the above equations, c_{ij} indicates the N-dimensional vector of samples corresponding to the i-th signal. N also denotes the number of samples. In the EMD process, the stopping criterion is met when the residual quantity r, defined in (9), becomes a monotonic function.

$$r = X - IMFi \quad (9)$$

where X represents the original signal, *IMFi* indicates the i-th intrinsic mode function extracted by applying EMD, and r denotes the residual quantity. The flowchart of the feature extraction method based on the HH transform technique is depicted in Fig. 3.

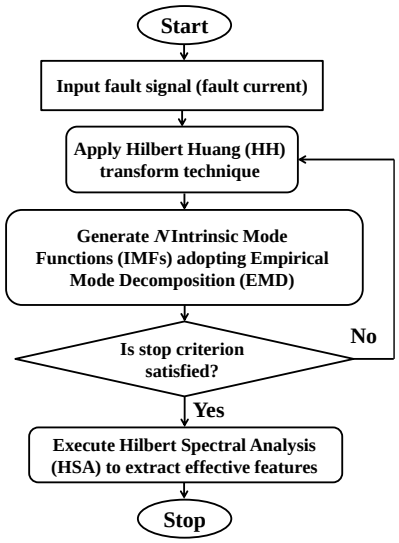

Figure 3. Flowchart of feature extraction method based on HH transform

III. Numerical Results and Discussion

A VSC-HVDC system with a length of 250km is selected as the case study and simulated in the MATLAB/Simulink R2018b on a machine with a 2.4GHz processor and 8GB of RAM. Three positive pole-to-ground (PPTG), negative pole-to-ground (NPTG), and positive-to-negative (PTG) faults are simulated at 24 equal distances of 10km with three fault resistances of 1Ω, 10Ω, and 100Ω at t=0.75s, and the DC-link currents are measured. Fig. 4 shows the DC-link currents corresponding to nine fault scenarios at a distance of 10km.

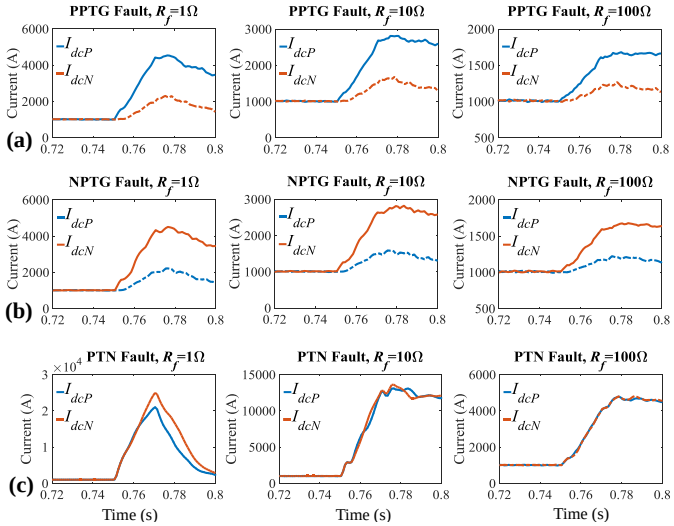

Figure 4. Signals corresponding to 9 fault scenarios at a distance of 10km

Next, the feature extraction scheme based on the HH transform is applied to the measured signals. Fig. 5 shows the obtained IMFs for one fault signal as an example. For this case, 16 IMFs are obtained. By applying the Hilbert function to the desired fault signal, the spectra containing RE and IM samples are acquired, as illustrated in Fig. 6. Likewise, one pair of RE and IM signals is obtained for each fault scenario at each distance, and the statistical indices defined in (6) to (8) are calculated for them. Accordingly, 1296 numerical values are obtained, as depicted in Fig. 7, and applied to train ANFIS. Before training ANFIS using the extracted features, it is necessary to compute the optimal parameters of the ANFIS utilizing the MCS algorithm. In this study, the Gaussian membership functions having two adjustable parameters, i.e., center (*c*) and width (*b*) defined in (10), are used to model ANFIS inputs.

$$\mu_{ij}\left(x_j\right)=exp\left\{\frac{-\left(x_j-c_{ij}\right)^2}{b_{ij}^2}\right\} \tag{10}$$

where c_{ij} and b_{ij} represent the parameters of the center and width of the membership functions corresponding to the *i*-th fuzzy rule and the *j*-th fuzzy variable, (*i*=1,2,...,*m* and *j*=1,2,...,*n*), respectively; where *m* and *n* indicate the number of fuzzy rules and input variables, respectively. In the ANFIS optimization process, the optimal parameters of the premise and consequence layers are obtained by minimizing the mean squared error (MSE) defined in (11).

$$MSE=\frac{1}{m}\sum_{i=1}^{m}\left(y_i-\hat{y}_i\right)^2 \tag{11}$$

where y_i and $\hat{y}_i$ denote the real and estimated values of the output of the *i*-th fuzzy rule, respectively. y_i is defined as follows:

$$y_i=\mathbf{x}^{\mathbf{T}}\pi_i \tag{12}$$

where $\mathbf{x}=\left[x_1 x_2 \cdots x_n\right]$ and $\boldsymbol{\pi}_i=\left[p_i^1\ p_i^2 \cdots p_i^n\right]$ represent the input and conclusion vectors corresponding to the *i*-th fuzzy rule, respectively. Interested readers are referred to [30] for more details about the ANFIS optimization process. By determining the optimal parameters of ANFIS, the membership functions corresponding to each input are obtained, as shown in Fig. 8. Additionally, the converged MSEs after 400 iterations of the ANFIS training algorithms are plotted in Fig. 9.

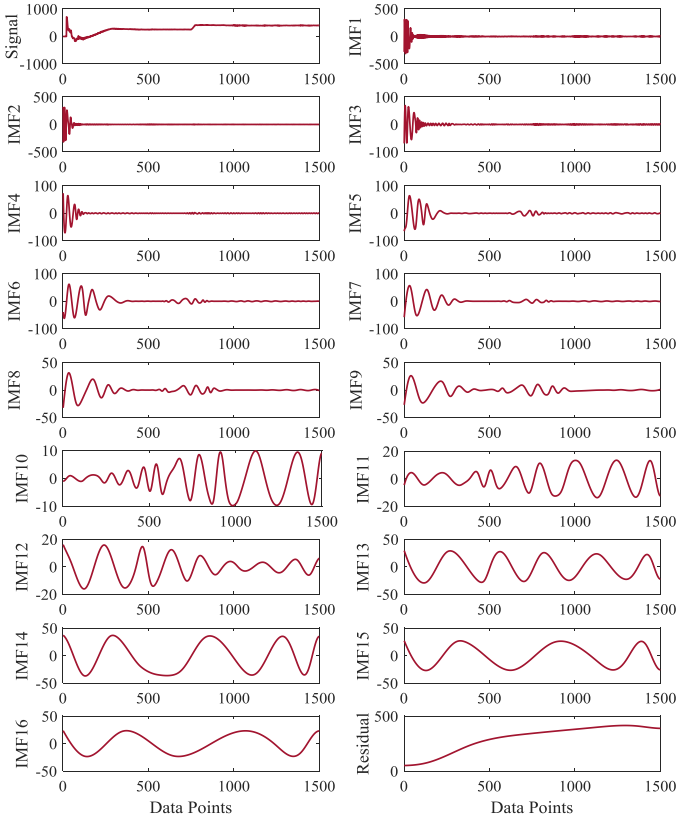

Figure 5. The IMFs corresponding to the PPTG fault scenario with R_f=100Ω at a distance of 10km

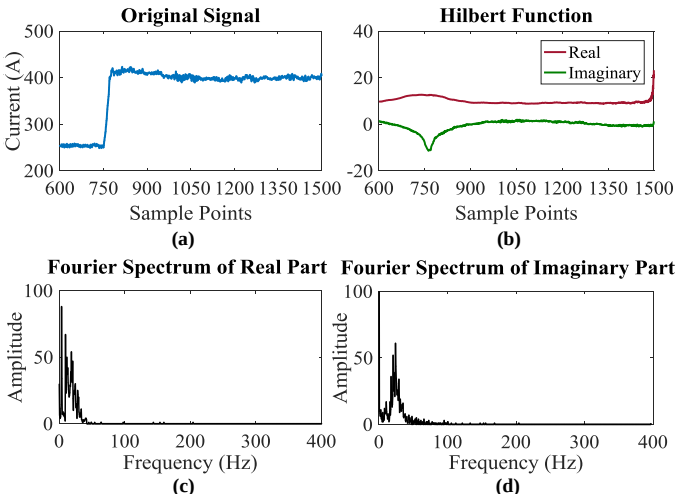

Figure 6. (a) the original fault signal, (b) real and imaginary spectra, and the Fourier spectra corresponding to the (c) real and (d) imaginary signals for the PPTG fault scenario with R_f=100Ω at a distance of 10km

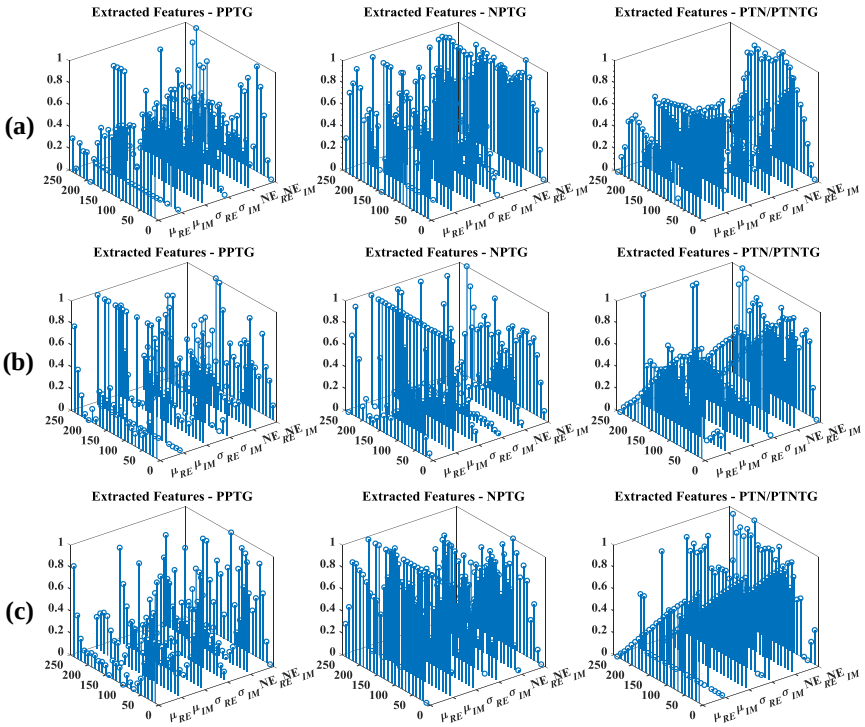

Figure 7. The extracted features by Hilbert-Huang transform technique, (a) R_f=1Ω, (b) R_f=10Ω, and (c) R_f=100Ω

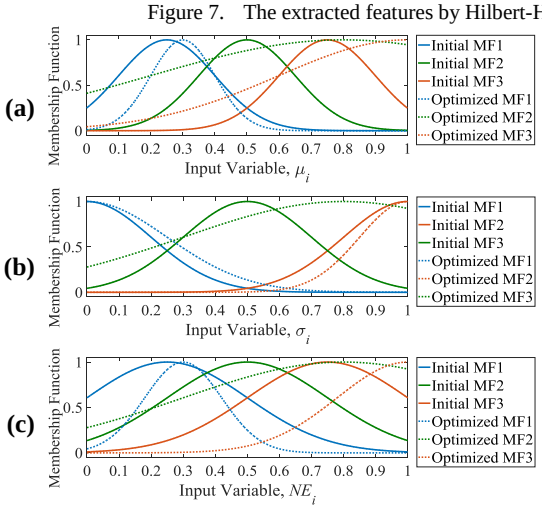

Figure 8. The initial and MSC-based optimized membership functions

For a better comparison, two conventional LSE and GD methods are also applied for ANFIS training, and their convergence trends are depicted in Fig. 9. To compare the ANFIS training methods, evaluation metrics defined in (13) to (16) are calculated for each model.

$$MSE = \frac{1}{N_s}\sum_{i=1}^{N_s}\left(T_i - O_i\right)^2 \tag{13}$$

$$RMSE = \sqrt{\frac{1}{N_s}\sum_{i=1}^{N_s}\left(T_i - O_i\right)^2} \tag{14}$$

$$R = \sqrt{1-\frac{\sum_{i=1}^{N_s}\left(T_i - O_i\right)^2}{\sum_{i=1}^{N_s}\left(T_i\right)^2}} \tag{15}$$

$$\text{Accuracy}\% = \frac{N_{CE}}{N_s}\times 100 \tag{16}$$

where T_i and O_i denote the target and output sampled data, respectively. Furthermore, N_{CE} and N_s represent the number of correctly estimated and initial sampled data, respectively.

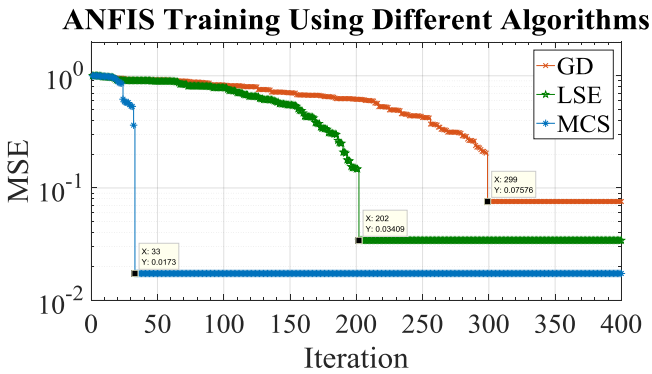

Figure 9. The convergence trends of the ANFIS training algorithms

For fault classification, nine fault cases (three fault types with three fault resistance values) by assigned identification codes 1 to 9, according to TABLE I, are considered. For training and testing ANFIS, a data set consisting of 1296 samples corresponding to the nine fault scenarios is constructed and applied to the optimized ANFIS. The training and testing results of ANFIS for fault classification are given in Fig. 10. In addition, the statistical indices obtained during the fault classification procedure are listed in TABLE II. In the next step, to locate the fault employing the proposed model, the extracted features shown in Fig. 7 are applied for training and testing the ANFIS. The results are presented in Fig. 11. Furthermore, TABLE III lists the statistical indices

corresponding to the ANFIS training and testing tasks in the fault location phase. For a better comparison, the results of the proposed ANFIS model based on the HH transform technique are compared with other fault location estimation models proposed in the literature in TABLE IV. This comparison is conducted in terms of the convergence speed of the ANFIS optimization algorithm, the best value obtained for the objective function, and execution time. The results presented in TABLE IV reveal that the proposed HHT-MCS-ANFIS model can locate faults more accurately due to the global minimization of the estimation error. In addition, faster convergence of the MCS algorithm leads to considerably reduce the execution time of the estimation model.

TABLE I. IDENTIFICATION CODES CORRESPONDING TO FAULT CASES

Fault Case		Label	Identification Code (IC)
PPTG	R_f=1Ω	PPTGR1	1
	R_f=10Ω	PPTGR10	2
	R_f=100Ω	PPTGR100	3
NPTG	R_f=1Ω	NPTGR1	4
	R_f=10Ω	NPTGR10	5
	R_f=100Ω	NPTGR100	6
PTN	R_f=1Ω	PTNR1	7
	R_f=10Ω	PTNR10	8
	R_f=100Ω	PTNR100	9

TABLE II. STATISTICAL ANALYSIS OF THE ANFIS-BASED FAULT CLASSIFIERS

ANFIS-based Classifier	MSE		RMSE		R		Accuracy%	
	Training	Testing	Training	Testing	Training	Testing	Training	Testing
GD-HHT	2.39209	3.96177	1.54664	1.99042	0.8802	0.8197	89.04	88.96
LSE-HHT	1.46141	2.84155	1.20889	1.68569	0.8955	0.8426	90.83	90.48
MCS-HHT	**0.25689**	**1.10965**	**0.50685**	**1.05340**	**0.9805**	**0.9136**	**97.53**	**97.37**

TABLE III. STATISTICAL ANALYSIS OF THE ANFIS-BASED FAULT LOCATORS

ANFIS-based Locator	MSE		RMSE		R		Accuracy%	
	Training	Testing	Training	Testing	Training	Testing	Training	Testing
GD-HHT	0.87976	0.89308	0.93796	0.94503	0.79012	0.78902	88.11	87.86
LSE-HHT	0.44920	0.46038	0.67023	0.67852	0.79885	0.80442	91.47	91.33
MCS-HHT	**0.04774**	**0.0.4939**	**0.21851**	**0.22226**	**0.83312**	**0.83971**	**98.45**	**98.39**

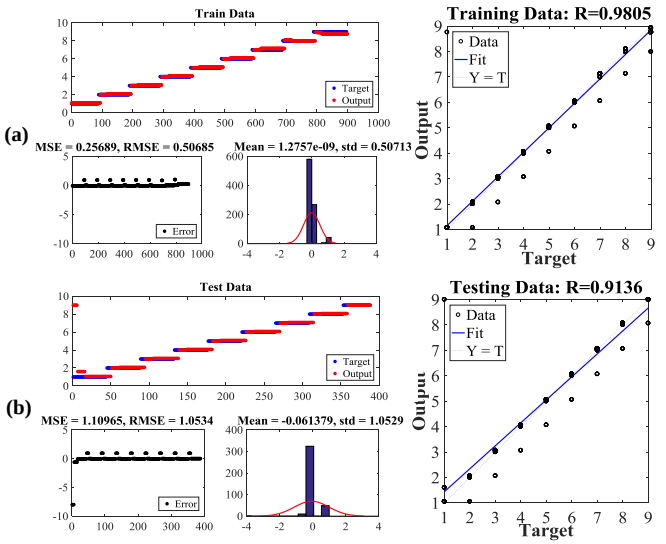

Figure 10. (a) Training and (b) testing of the HHT-MCS-ANFIS classifier

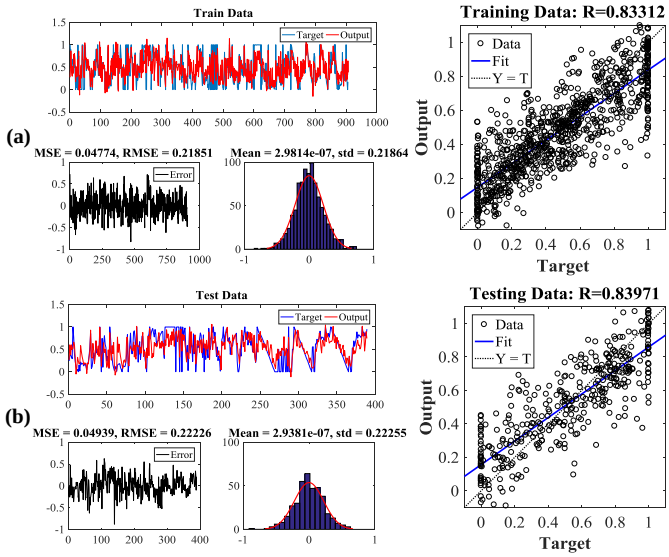

Figure 11. (a) Training and (b) testing of the HHT-MCS-ANFIS locator

TABLE IV. THE COMPARATIVE STUDY RESULTS

ANFIS Optimization Algorithm	The Converged MSE Value (Best Result)	Maximum Iteration Until Convergence (Best Result)	Execution Time (sec) (Best Result)
CDWPSO [17]	0.0592	Not mentioned	Not mentioned
LS+BP [17]	0.1839	Not mentioned	Not mentioned
LS+BP [15]	0.2445	~365	Not mentioned
PSO [15]	0.0546	~280	Not mentioned
GA [15]	0.0378	~215	Not mentioned
CDWPSO [15]	0.0255	~50	Not mentioned
NSGA-II [15]	0.0197	~30	Not mentioned
This Work (GD)	0.0757	299	66.142
This Work (LSE)	0.0340	202	35.986
This Work (MCS)	**0.0173**	**33**	**8.215**

I. Conclusions

An intelligent model was proposed in this paper to detect, classify, and locate faults in VSC-HVDC networks. The proposed model was designed based on the optimized ANFIS, and the features extracted by the Hilbert-Huang transform method were used for ANFIS training and testing. The modified cuckoo search (MCS) algorithm was utilized to determine the optimal parameters of ANFIS. For comparison, two conventional methods, LSE and GD, were exploited to train ANFIS. Numerical results demonstrate that the proposed estimation model can classify the fault with an accuracy of 97.37%, and the precision of the fault location estimation is 98.39%. The final value of the objective function MSE obtained using the proposed MSC-optimized ANFIS framework is 0.0173, which reveals a reduction of 77.14% and 49.11% compared to the GD and LSE algorithms, respectively. In addition, the final MSE value is reduced by 12.18% compared to the best result obtained in the literature (0.0197 corresponding to the NSGA-II optimization algorithm). Faster convergence during fewer iterations (33 iterations) compared to other ANFIS training methods is another advantage of the proposed MCS algorithm. This advantage affects the speed of fault diagnosis, classification, and location; hence, it allows the HVDC system operator to perform isolation and recovery actions for the faulty part of the network as quickly as possible.

References

[1] M. Muniappan, "A comprehensive review of DC fault protection methods in HVDC transmission systems," Prot. Control Mod. Power Syst., vol. 6, pp. 1–30, 2021.

[2] Q. Wang, Y. Yu, H. O. A. Ahmed, M. Darwish, and A. K. Nandi, "Fault detection and classification in MMC-HVDC systems using learning methods," Sensors, vol. 20, no. 16, pp. 1-19, August 2020.

[3] L. Yuansheng, W. Gang, and L. Haifeng, "Time-domain fault-location method on HVDC transmission lines under unsynchronized two-end measurement and uncertain line parameters," IEEE Trans. Power Deliv., vol. 30, no. 3, pp. 1031-1038, June 2015.

[4] J. Yan, C. Zhao, F. Zhang, and J. Xu, "The preemptive virtual impedance based fault current limiting control for MMC-HVDC," 8th Renewable Power Generation Conference, Shanghai, China, pp. 1-6, 24-25 October 2019.

[5] Q. Yang, S. L. Blond, B. Cornelusse, P. Vanderbemden, and J. Li, "A novel fault detection and fault location method for VSC-HVDC links based on gap frequency spectrum analysis," Energy Procedia, vol. 142, pp. 2243-2249, December 2017.

[6] W. Chen, D. Wang, D. Cheng, and X. Liu, "Travelling wave fault location approach for MMC-HVDC transmission line based on frequency modification algorithm," Int J. Electr. Power Energy Syst., vol. 143, p. 108507, December 2022.

[7] A. B. Soeth, P. R. F. de Souza, D. T. Custódio, and I. Voloh, "Traveling wave fault location on HVDC lines," 71st Annual Conference for Protective Relay Engineers, College Station, TX, USA, pp. 1-16, 26-29 March 2018.

[8] R. Muzzammel, "Traveling waves-based method for fault estimation in HVDC transmission system," Energies, vol. 12, no. 19, pp. 1-31, September 2019.

[9] D. Wang, J. Fu, M. Hou, F. Qiao, and M. Gao, "Novel travelling wave fault location principle for VSC-HVDC transmission line," Electr. Power Syst. Res., vol. 196, p. 107226, July 2021.

[10] B. Wang, L. Yang, and X. Dong, "Fault location method for high-voltage direct current transmission line using incident current travelling waves," J. Eng., vol. 2018, no. 15, pp. 1165-1168, October 2018.

[11] A. Fedorov, V. Petrov, O. Afanasieva, and I. Zlobina, "Limitations of traveling wave fault location," Ural Smart Energy Conference, Ekaterinburg, Russia, pp. 21-25, 13-15 November 2020.

[12] P. C. Fernandes, T. R. Honorato, F. V. Lopes, K. M. Silva, and H. N. G. V. Gonçalves, "Evaluation of travelling wave-based fault location methods applied to HVDC systems," Electr. Power Syst. Res., vol. 189, p. 106619, December 2020.

[13] S. K. Yellagoud, and P. R. Talluri, "Assessment of fault location methods for electric power distribution networks," 4th International Conference for Convergence in Technology, Mangalore, India, pp. 1-8, 27-28 October 2018.

[14] C. F. Mbey, V. J. F. Kakeu, A. T. Boum, and F. G. Y. Souhe, "Fault detection and classification using deep learning method and neuro-fuzzy algorithm in a smart distribution grid," J. Eng., vol. 2023, no. 11, pp. 1-19, November 2023.

[15] R. Rohani, A. Koochaki, and J. Siahbalaee, "Fault location in VSC-HVDC systems based on NSGA-II and discrete wavelet transform," Int. J. Renew. Energy Res., vol. 12, no. 3, pp. 1347- 1361, September 2022.

[16] M. Khadem, A. T. Eshlaghy, and K. F. Hafshejani, "Improving the performance of adaptive neural fuzzy inference system (ANFIS) using a new meta-heuristic algorithm," Int. J. Math. Model. Comput., vol. 12, no. 4, pp. 299-312, December 2022.

[17] R. Rohani, and A. Koochaki, "A hybrid method based on optimized neuro-fuzzy system and effective features for fault location in VSC-HVDC Systems," IEEE Access, vol. 8, pp. 70861-70869, April 2020.

[18] N. B. Roy, "Fault identification and determination of its location in a HVDC system based on feature extraction and artificial neural network," J. Inst. Eng. (India): B, vol. 102, pp. 351-361, 2021.

[19] L. Li, "Review of feature extraction methods for power equipment monitoring data," J. Comput. Commun., vol. 16, pp. 19-24, 2021.

[20] S. H. Syed, and V. Muralidharan, "Feature extraction using Discrete Wavelet Transform for fault classification of planetary gearbox – a comparative study," Appl. Acoust., vol. 188, pp. 108572, January 2022.

[21] M. Zuhaib, et al., "Faults feature extraction using discrete wavelet transform and artificial neural network for induction motor availability monitoring—internet of things enabled environment," Energies, vol. 15, no. 21, pp. 1-32, October 2022.

[22] R. Bajric, N. Zuber, G. A. Skrimpas, and N. Mijatovic, "Feature extraction using discrete wavelet transform for gear fault diagnosis of wind turbine gearbox," Shock Vib., vol. 2016, pp. 1-11, December 2016.

[23] N. Ahmed, A. A. Hashmani, S. Khokhar, M. A. Tunio, and M. Faheem, "Fault detection through discrete wavelet transform in overhead power transmission lines," Energy Sci. Eng., vol. 11, no. 11, pp. 4181-4197, November 2023.

[24] A. I. Salehi, and N. Ghaffarzadeh, "Fault detection and classification of VSC-HVDC transmission lines using a deep intelligent algorithm," Int. J. Res. Technol. Electr. Ind., vol. 1, no. 2, pp. 161-170, September 2022.

[25] N. Prabhu, M. K. Arora, and R. Balasubramanian, "Wavelet based feature extraction techniques of hyperspectral data," J. Indian Soc. Remote. Sens., vol. 444, pp. 373-384, 2016.

[26] Y. Lim, J. Kwon, and H. S. Oh, "Principal component analysis in the wavelet domain," Pattern Recognit., vol. 119, p. 108096, November 2021.

[27] X. Yang, and S. Deb, "Cuckoo Search via Lévy flights," World Congress on Nature & Biologically Inspired Computing, Coimbatore, India, pp. 210-214, 09-11 December 2009.

[28] T. T. Nguyen, D. N. Vo , Ng. V. Quynh, and L. V. Dai, "Modified cuckoo search algorithm: a novel method to minimize the fuel cost," Energies, vol. 11, no. 6, pp. 1-27, May 2018.

[29] X. Zhu, S. Li, Y. Guo, X. Chen, C. He, and J. Deng, "Novel wavefront detection and fault location method based on Hilbert-Huang transform for long HVDC transmission lines," Electr. Power Syst. Res., vol. 211, p. 108213, October 2022.

[30] D. Karaboga, and E. Kaya, "Adaptive network based fuzzy inference system (ANFIS) training approaches: a comprehensive survey," Artif. Intell. Rev., vol. 52, pp. 2263-2293, 2019.